Journal of Inflammation Research

Dovepress
Taylor & Francis Group

Open Access Full Text Article

ORIGINAL RESEARCH

Protective Effect of Xihuang Pill on Immune Checkpoint Inhibitors-Related Myocarditis in a Mouse Model by Regulating the HIF-1 Signaling Pathway

Bo Cao[1,*], Huijuan Xie[1,*], Jing Xu[2], Nuoxian Yu[3], Zhuo Man[4], Wenwen Zhao[4], Guohui Li[2], Chunyu Li[2], Li Han[1]

[1]State Key Laboratory of Southwestern Chinese Medicine Resources, School of Pharmacy, Chengdu University of Traditional Chinese Medicine, Chengdu, 611137, People's Republic of China; [2]National Cancer Center/National Clinical Research Center for Cancer/Cancer Hospital, Chinese Academy of Medical Sciences and Peking Union Medical College, Beijing, 100021, People's Republic of China; [3]Department of Pharmacy, The First Hospital of China Medical University, Shenyang, 110001, People's Republic of China; [4]SCIEX China, Beijing, 100015, People's Republic of China

*These authors contributed equally to this work

Correspondence: Chunyu Li; Li Han, Email licy@cicams.ac.cn; hanliyx@163.com

Background: Immune checkpoint inhibitor (ICIs)-associated cardiotoxicity is a significant cause of immune-related adverse events and mortality in cancer immunotherapy, lacking effective preventative or therapeutic strategies. Xihuang Pill (XHW), a traditional Chinese medicine with established anti-inflammatory properties and clinical use in cancer treatment and adverse event mitigation, merits investigation for its efficacy against ICIs-induced cardiac toxicity.

Purpose: To investigate XHW's therapeutic effects on Immune checkpoint inhibitors (ICIs)-associated cardiotoxicity and its underlying mechanisms.

Methods: This study utilized mass spectrometry technology to identify the chemical components in XHW. The experimental model for ICIs-associated myocarditis was generated in BALB/c mice by immunizing them with murine cardiac troponin I (cTnI) peptide and administering anti-programmed death 1 (PD-1) antibodies to mice. Mice received varying XHW dosages (0.39, 0.78, and 1.56 mg/kg). Myocardial contractility and plasma cardiac injury markers (CK, CK-MB) were assessed. Metabolomics and transcriptomics identified key signaling pathways modulated by XHW, validated via real-time quantitative PCR (QT-PCR). In addition, a correlation analysis was conducted between key genes and differential metabolites.

Results: Mass spectrometry identified 171 components in XHW. Pharmacological studies demonstrated that XHW improved cardiac contractility, reduced plasma cardiac injury biomarkers, and attenuated myocardial injury in the myocarditis model. Integrated metabolomic and transcriptomic analyses revealed that XHW primarily modulates the HIF-1 signaling pathway, significantly upregulating *HIF-1* mRNA expression and downregulating the mRNA expression of *Nppa, Angpt1, Angpt2*, and *Trf*. Correlation analysis identified significant associations between 16 metabolites, including 13-tetradecynoic acid, 1-pentadecanoylglycerol, and arginyl-glycyl-aspartic acid, and these genes.

Conclusion: These findings suggest that XHW may alleviate ICIs-associated myocarditis via HIF-1 signaling pathway, offering a promising therapeutic approach for ICIs-related cardiotoxicity.

Keywords: Xihuang pill, immune checkpoint inhibitors, cardiotoxicity, metabolomics, transcriptomic

Introduction

Over the past decade, immune checkpoint inhibitors (ICIs) therapy has revolutionized the treatment paradigm for various cancers, marking the third wave of innovation in the field of tumor therapy, following cytotoxic chemotherapy and targeted drug therapy.[1] Currently, ICIs used in clinical practice mainly include the programmed death-1 (PD-1) inhibitors,

Received: 10 March 2025
Accepted: 21 August 2025
Published: 7 November 2025

programmed death ligand 1 (PD-L1) inhibitors, and cytotoxic T-lymphocyte-associated antigen 4 (CTLA-4) inhibitors.[2] However, nearly all ICIs can cause excessive activation of the immune system, potentially leading to immune-related adverse events (irAEs), such as skin toxicity, endocrine toxicity, pneumonia, hepatitis, and cardiotoxicity.[3,4] Among them, ICIs-associated cardiac toxicity is a rare but severe type of irAEs.[5] The clinical symptoms encompass myocarditis, arrhythmia, and heart failure.[6] The specific mechanism by which ICIs induce cardiac toxicity events remains unclear. Current research suggests that it may be due to T cells recognizing the same antigen in myocardial and tumor tissues, or T cells cross-recognizing different antigens with high homology.[7,8] Currently, high-dose steroid pulse therapy is primarily used for treating ICIs-related myocarditis. However, in clinical diagnosis and treatment, it has been observed that some patients may experience reduced clinical benefits due to hormone resistance, which may ultimately lead to adverse cardiovascular events.[9] Therefore, it is urgent to search effective therapies to prevent and treat ICIs-associated myocarditis.

Previous clinical practice and multiple studies have demonstrated that traditional Chinese medicine (TCM) is effective in reducing related adverse reactions and improving patients' quality of life in fields such as tumor chemotherapy, targeted therapy and immunotherapy.[10–12] Currently, there is relatively little research on the prevention and treatment of ICIs-related cardiac injury with TCM. However, TCM has achieved important results in tumor cardiology, especially in chemotherapy-induced cardiac toxicity, which has certain guiding significance for the prevention and treatment of ICIs-associated cardiac injury.[13,14]

Xihuang Pill (XHW) is a blend of four herbal ingredients: *Calculus Bovis* (derived from *Bos taurus domesticus* Gmelin), *Moschu*s (sourced from *Moschus berezovskii* Flerov), *frankincense* (derived from *Boswellia carterii* Birdw.) and *Myrrh* (obtained from *Commiphora myrrha* Engl).[15,16] XHW has been extensively employed as an adjuvant therapy for malignant tumors in China, capable of enhancing the effectiveness of radiotherapy and chemotherapy, minimizing adverse reactions, and elevating the quality of life for patients.[17] Recent studies indicate that both XHW and its constituent herbs exhibit anti-inflammatory properties.[18,19] Furthermore, key components within XHW, including Boswellic acid, ursolic acid, acetyl-11-keto-beta-boswellic acid, and 11-keto-beta-boswellic acid, possess a protective effect on the heart.[20–23] Nevertheless, it remains uncertain whether XHW can notably alleviate ICIs-related cardiac toxicity, and the precise mechanism underlying its therapeutic efficacy remains unclear. This study explored XHW to alleviate ICIs-related cardiotoxicity, which may provide a new strategy for the treatment of ICIs-induced cardiac dysfunction.

Materials and Methods

Reagents and Drugs

Xihuang Pill (Lot#2112015) was purchased from Zhejiang Tianyitang Pharmaceutical Co., Ltd. (China). The anti-mouse PD-1 monoclonal antibody (clone: RMP1-14, Cat #: BP0146) was sourced from BioXCell (USA). Murine cardiac troponin I (TnI) peptide (sequence: HARVDKVDEERYDVEAKVTKNITEIADLTQKIYDLRGKFKRPTLRRVRIS) was synthesized by Nanjing Jietai Biotechnology Co., Ltd. (Cat #: JT-177503, Nanjing, China). Freund's adjuvant (Cat #: 642852) was purchased from Beijing Solarbio Science & Technology Co.,Ltd. Other chemicals and reagents were commercially sourced.

UPLC-MS/MS Settings

We utilized the Exion LC (SCIEX, MA, USA) and SCIEX Zeno TOF 7600 (SCIEX, MA, USA) high-resolution mass spectrometry systems. Additionally, we employed a Luna Omega Polar C18 (100x2.1mm, 1.6um) chromatographic column. The mobile phase for liquid chromatography consisted of an aqueous solution containing 0.1% formic acid (A), along with a mixture of 50% formic acid and 50% acetonitrile (B). The elution gradient was as follows: 0–1 minute, 5% B; 1–2 minutes, 25% B; 2–35 minutes, 25–50% B; 35–52 minutes, 50–95% B; 52–57 minutes, 95% B; 57–60 minutes, 5% B. The total running time was 60 minutes, with a flow rate of 0.2 mL/min. We employed the electrospray ionization (ESI) method in both positive and negative ion modes, utilizing multiple reaction monitoring (MRM) channels.

Animal Experimental Plan

Based on relevant literature,[24,25] a sample size of 6 mice per group was selected. This study established 5 groups, each consisting of 6 mice, totaling 30 male BALB/c mice aged six weeks (License No.: SCXK 2019–0010), supplied by SPF (Beijing) Biotechnology Co., Ltd. The mice were maintained in a specific pathogen-free (SPF) environment at 25 ± 2°C and 50 ± 10% relative humidity, under a 12-hour light-dark cycle.

Experimental Design and Animal Treatment

All mice, except those in the vehicle group, received subcutaneous immunizations with 250 μg murine cardiac TnI peptide in complete Freund's adjuvant on days 0 and 7. Beginning on day 8, mice received intraperitoneal injections of anti-mouse PD-1 (10 mg/kg) every 2 days for five administrations to induce ICIs-associated myocarditis.[26]

Mice were randomly assigned to five groups (n=6 per group): (I) Vehicle group (vehicle-treated group); (II) Model group (10 mg/kg anti-mouse PD-1); (III) XHW-L (10 mg/kg anti-mouse PD-1 + 0.39 mg/kg/day XHW, p.o).; (IV) XHW-M (10 mg/kg anti-mouse PD-1 + 0.78 mg/kg/day XHW, p.o).; (V) XHW-H (10 mg/kg anti-mouse PD-1 + 1.56 mg/kg/day XHW, p.o). The selection of drug dosages is based on the outcomes of initial experiments. The conversion of human-equivalent doses to those suitable for mice is calculated using body surface area. The mice were administered low, medium, and high doses of XHW at 0.39 g/kg, 0.78 g/kg, and 1.56 g/kg, respectively, which correspond to half, equal to, and double the clinical equivalent dose of 6 g/day.[27] XHW was crushed into a fine powder and then suspended in a 0.5% sodium carboxymethylcellulose (CMC-Na) solution. Anti-mouse PD-1 was diluted to 1mg/mL with PBS. The mice in the vehicle group were administered an equal volume of 0.5% CMC-Na. XHW administration commenced on day 8 and continued for 14 consecutive days. Echocardiography was conducted on day 21, after which mice were euthanized with deep isoflurane (5%) anesthesia, and cardiac tissue was harvested.

Echocardiography

Transthoracic echocardiography was conducted on day 21 using a high-frequency scan probe on all experimental animals. The mice were anesthetized and maintained with isoflurane and oxygen throughout the procedure. Fractional shortening (FS) and left ventricular ejection fraction (LVEF) were measured following established protocols. The measurements were performed by a blinded investigator, and the data was analyzed using Vevo Analysis software.

Biochemical Testing for Myocardial Injury

50 μL of plasma was taken, melted on ice, diluted fourfold with normal saline, and then placed into the sampling frame in order. The enzyme activities of creatine kinase (CK) and creatine kinase-MB (CK-MB) in the plasma of mice from each group were detected using an automatic biochemical analyzer.

Plasma Metabolomics Analysis

Fifty microliters of the sample was mixed with 300 microliters of extraction solution (ACN: Methanol = 1:4, V/V) containing internal standards in a 2 mL microcentrifuge tube. The mixture was vortexed for 3 min and centrifuged at 12,000 rpm for 10 min at 4°C. 200 μL of the supernatant was collected and stored at −20°C for 30 min before a second centrifugation at 12,000 rpm for 3 min at 4°C. Finally, 180 μL of the supernatant was analyzed by LC-ESI-MS/MS using an ExionLC AD UPLC system coupled with a QTRAP® mass spectrometer. The LC-ESI-MS/MS system was operated under the following analytical conditions: A Waters ACQUITY UPLC BEH C18 column (1.8 μm, 2.1 mm×100 mm) was utilized with a column temperature set at 40°C. The analysis employed a flow rate of 0.4 mL/min and a 2 μL injection volume. The mobile phase was a mixture of water and acetonitrile, each containing 0.1% formic acid. Time-of-flight mass spectrometry (TOF MS) parameters were set as follows: m/z 50–1000, 200 ms accumulation time, and dynamic background subtraction enabled.

Differential metabolites were identified using a two-group comparison based on variable importance in projection (VIP) scores (VIP > 1) and statistically significant p-values ($P < 0.05$, Student's t-test). Unsupervised principal component analysis (PCA) visualized overall sample relationships. Orthogonal partial least squares discriminant

analysis (OPLS-DA), performed using the MetaboAnalystR R package, yielded VIP scores, score plots, and permutation plots (200 permutations) to mitigate overfitting. Data were log2-transformed and mean-centered prior to OPLS-DA. Identified metabolites were annotated using the Kyoto Encyclopedia of Genes and Genomes (KEGG) database and subsequently mapped to KEGG pathways. Further metabolic analyses were conducted on the Metware Cloud Platform.

RNA Sequencing

The heart tissue samples were sent to Shanghai NovelBio Co., Ltd (http://www.novelbio.com/, Shanghai, China) for RNA sequencing (RNA-seq). Total RNA was extracted from samples using Trizol reagent (Invitrogen), and its quality was assessed using an Agilent 2200 Bioanalyzer. Only samples with an RNA Integrity Number (RIN) exceeding 7.0 were used for cDNA library construction with the VAHTS Universal V6 RNA-seq Library Prep Kit for Illumina (Vazyme). Raw sequencing reads underwent quality control, including adapter and low-quality read trimming, generating clean reads. These clean reads were aligned to the mouse genome (mm10_Ensembl100) using HISAT2. Gene counts were quantified using HTSeq, and gene expression levels were calculated using fragments per kilobase of transcript per million mapped reads (FPKM). Differentially expressed genes (DEGs) were identified using DESeq2, with a significance threshold of $|\log2(\text{fold change})| > 0.58$ (corresponding to a fold change > 1.5 or < 0.667), $P < 0.05$, and false discovery rate (FDR) < 0.05. KEGG pathway enrichment analysis, employing Fisher's exact test ($P < 0.05$), identified significantly enriched pathways associated with the DEGs. Additional gene analyses were performed using the Metware Cloud Platform (https://sc.novelbrain.com).

Real-Time Quantitative PCR

Total RNA was extracted from mouse heart tissue using the RNApure Fast Tissue&Cell Kit (Cwbio, Cat #: CW0599S, Taizhou, China) according to the manufacturer's instructions. The RNA concentrations were normalized and then reverse-transcribed into cDNA using the HiFiScript All-in-one RT Master Mix for qPCR (Cwbio, Cat #: CW3371M, Taizhou, China). Quantitative real-time PCR assays were carried out using an Applied Biosystems QuantStudio 5 with total RNA and the SuperStar Universal SYBR Master Mix (Cwbio, Cat #: CW3390M, Taizhou, China). Primers were designed using NCBI/Primer3 plus software and can be found in Table S1. The qPCR signals were quantified using the ΔΔCt relative quantification method with β-actin as the reference gene.

Correlation Analysis

This study employed Pearson correlation analysis to assess the association between differential metabolites and differential metabolites. Correlation coefficients were computed using the cor function (R base package; Hmisc) for each sample pair.

Statistical Analysis

Statistical analysis was performed using GraphPad Prism 8.0. Data, presented as mean ± standard deviation, were compared using one-way ANOVA. Statistical significance was defined as $p < 0.05$ for between-group comparisons.

Results

Identification of XHW Compounds

We developed a UPLC-MS/MS method to identify the chemical components in XHW and conducted an analysis of the chemical substances present in XHW extract samples. The typical characteristics of total ion chromatography for XHW in both positive and negative signal modes are illustrated in Figure 1. Leveraging local databases, fragment ion retention times, mass charge ratios, and pertinent literature on four herbs containing XHW, we identified 171 components within XHW through rigorous analysis (Table S2).

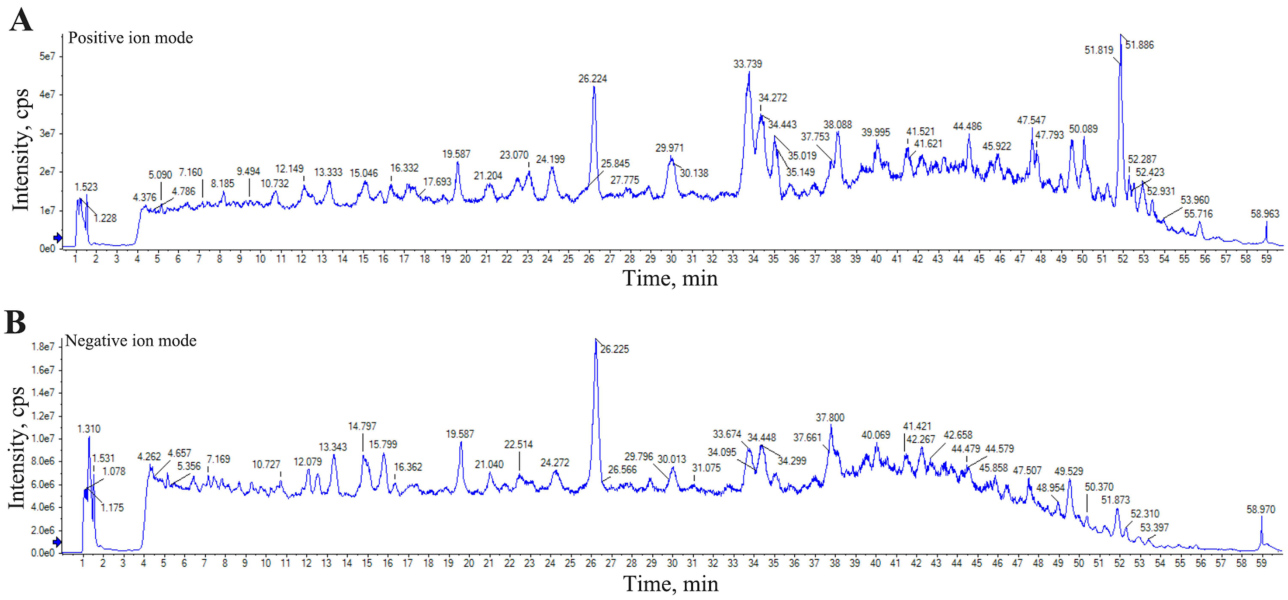

Figure 1 Total ion chromatogram of Xihuang Pill (XHW) in positive (**A**) and negative (**B**) ion modes.

XHW Alleviates ICIs-Related Cardiotoxicity in Mice

To examine the involvement of XHW in ICIs-related cardiotoxicity, we established a mouse model as described above. The experimental design is illustrated in Figure 2A. On the 21st day, echocardiography was utilized to evaluate both the function of the left ventricle (Figure 2B). The findings indicated that both the left ventricular ejection fraction and fraction shortening were notably decreased in the model group when compared to the vehicle group. The XHW-M and XHW-H groups receiving XHW, instead of the XHW-L group being given XHW, demonstrated a significant enhancement in left ventricular function (Figure 2C and D). In addition, the plasma levels of CK and CK-MB were measured to assess myocardial injury. As illustrated in Figure 2E and F, the induction of ICIs-related cardiotoxicity resulted in a significant increase in CK and CK-MB levels compared to the vehicle group. Administration with XHW of 1.56 g/kg partially reversed CK levels, while the doses of XHW 0.39 g/kg and 0.78 g/kg significantly reduced CK levels. Furthermore, XHW in 0.39 g/kg, 0.78 g/kg and 1.56 g/kg significantly decreased CK-MB levels. The HE staining results of myocardial tissue from the vehicle, model, and XHW-M groups are presented in Figure 2G. Compared to the vehicle group, the myocardial tissue of the model group exhibited varying degrees of inflammatory infiltration induced by ICIs. However, when compared to the model group, XHW ameliorated the inflammatory infiltration. These findings suggest that XHW has the potential to mitigate ICIs-related cardiotoxicity in mice.

Effects of XHW on Metabolome in ICIs-Induced Cardiotoxicity Mice

To explore the metabolic mechanism by which XHW improves ICIs-related cardiotoxicity, we conducted untargeted metabolomic studies on plasma samples. Principal component analysis (PCA) was applied to observe true differences between groups. PCA score scatter plots are shown in Figure 3A (ESI-) and Figure 3B (ESI+) respectively. Quality control (QC) samples showed consistent concentration, demonstrating instrument stability throughout the experiment. PCA revealed clear separation between vehicle, model, and XHW groups, highlighting significant metabolic differences among the three.

To further investigate differential metabolites among the vehicle, model, and XHW groups, orthogonal partial least squares discriminant analysis (OPLS-DA) was used for classification and discrimination. OPLS-DA scores clearly distinguished the vehicle, model, and XHW groups (Figure 3C and D). The model parameters (vehicle vs model group: $R^2X = 0.375$, $R^2Y = 0.993$, $Q^2 = 0.858$, and $P < 0.005$; model vs XHW group: $R^2X = 0.311$, $R^2Y = 0.999$, $Q^2 = 0.845$, and $P < 0.005$) demonstrate the OPLS-DA model's strong interpretability and predictive power (Figure 3E and F). Metabolites deemed to have a variable

 https://doi.org/10.2147/JIR.S527372

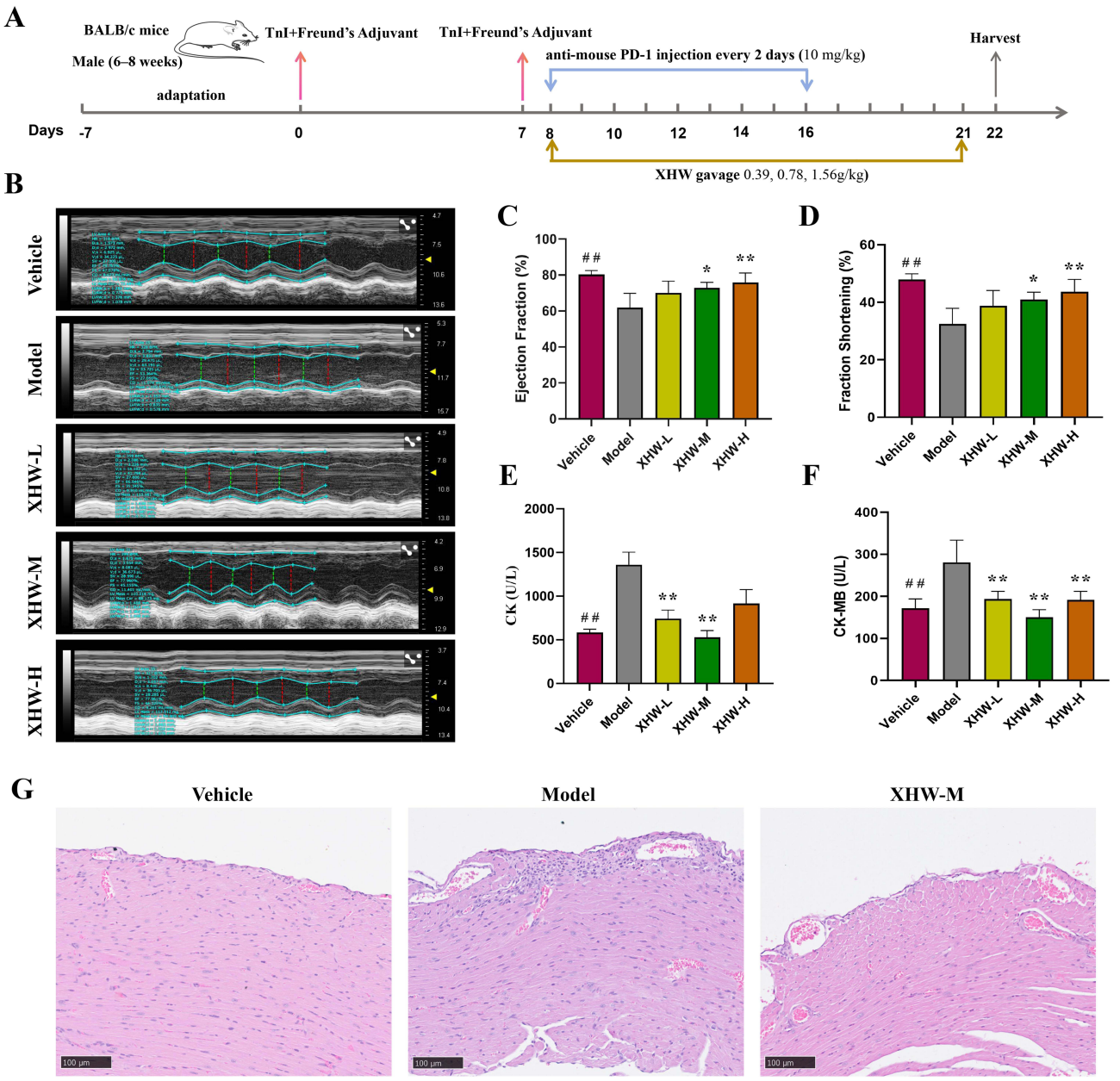

Figure 2 XHW improved inhibitor (ICIs)-related myocarditis. (**A**) Administration regimen schematic for XHW treatment of ICIs-related myocarditis. (**B**) Representative images of mouse echocardiography from the different intervention groups. (**C**), (**D**) Analyses of ejection fraction (EF) and fraction shortening (FS). (**E**), (**F**) Analyses of plasma levels of creatine kinase (CK) and creatine kinase-MB (CK-MB). (**G**) Representative images of HE staining from the vehicle, model, and XHW-M groups. Results are expressed as mean ± standard deviation (SD) (n = 6 per group). $^{\#\#}P < 0.01$, vehicle vs model; $^{*}P < 0.05$; $^{**}P < 0.01$, model vs XHW groups.

importance in projection (VIP) score of ≥ 1.0, a P-value of < 0.05, and a fold change of either ≥ 1.5 or ≤ 0.67 were classified as differential metabolites (Figure 4A, D and Figure S1)). In total, 189 differential metabolites were identified when comparing the vehicle group with the model group, while 152 were found when comparing the model group to the XHW group. Notably, when comparing the model group to the XHW group, the levels of 111 metabolites exhibited an increase, whereas 41 metabolites showed a decrease. To facilitate a clearer observation of metabolite changes, a qualitative and quantitative analysis was performed on the primary identified metabolites from each group.

To enhance the identification of pertinent metabolic pathways through which XHW mitigates cardiotoxicity associated with ICIs, differential metabolites were submitted to the KEGG database for the construction and analysis of metabolic pathways. Results revealed key pathways including taurine and hypotaurine metabolism, ascorbate and aldarate metabolism, sphingolipid metabolism, HIF−1 signaling pathway, and Sphingolipid signaling pathway (Figure 4E and Table S3).

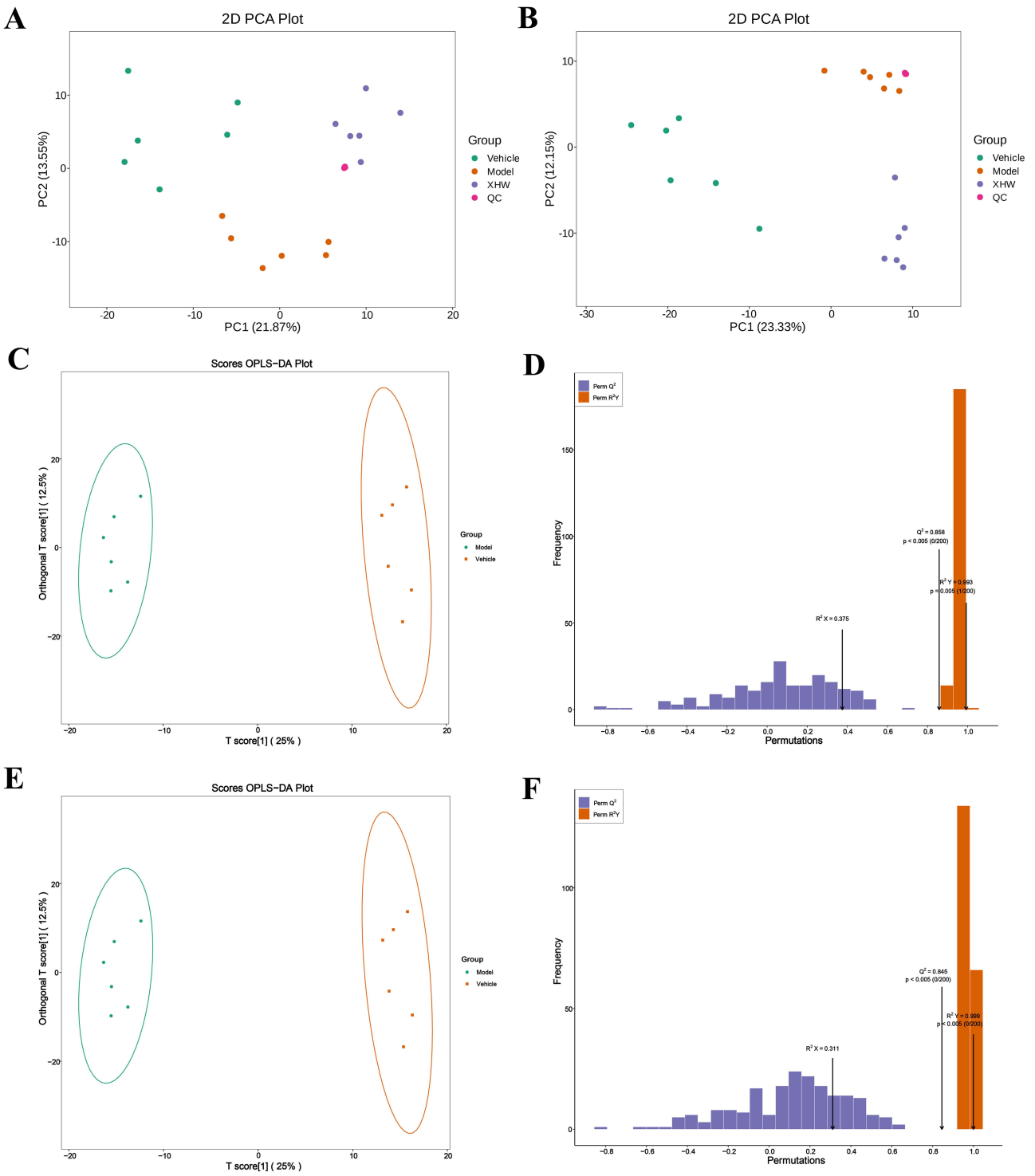

Figure 3 Metabolic changes in the plasma caused by XHW in ICIs-related myocarditis mice. (**A**), (**B**) Principal component analysis (PCA) score plots from the vehicle, model and XHW groups in negative electrospray ionization source (ESI-) mode and positive electrospray ionization source (ESI+), respectively. (**C**), (**E**) Orthogonal partial least squares discriminant analysis (OPLS-DA) score plots of the vehicle and model groups, the model and XHW groups. (**D**), (**F**) OPLS-DA model test chart of the vehicle and model groups, the model and XHW groups.

Effects of XHW Supplementation on Cardiac Transcriptome

To explore the biological mechanism of XHW in improving ICIs-related myocarditis, RNA sequencing analysis was performed on heart samples from the vehicle, model, and XHW groups. The PCA analysis indicated a clear separation among the vehicle, model, and XHW groups, with the XHW group being nearer to the vehicle group (Figures 5A).

https://doi.org/10.2147/JIR.S527372

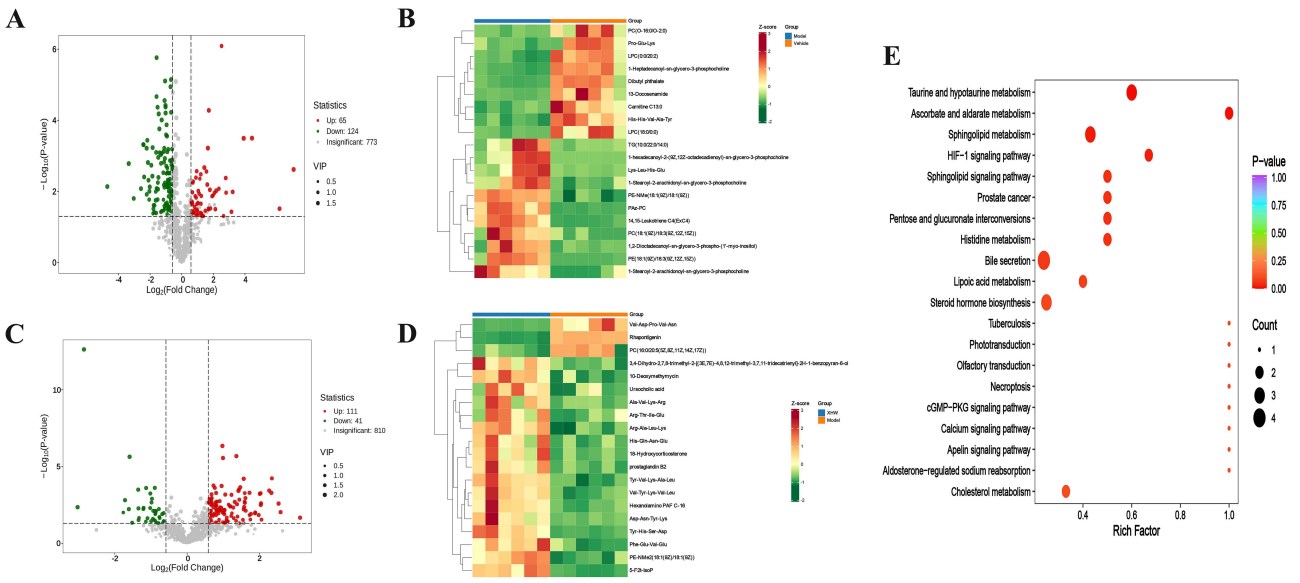

Figure 4 The metabolic characteristics induced by XHW in ICIs-related myocarditis mice. (**A**) Volcano Plot Analysis between the vehicle and model groups. (**B**) Hierarchical clustering heatmap of differential metabolites between the vehicle and model groups. (**C**) Volcano Plot Analysis between the model and XHW groups. (**D**) Hierarchical clustering heatmap of differential metabolites between the model and XHW groups. (**E**) Metabolic pathways influenced by XHW based on the Kyoto Encyclopedia of Genes and Genomes (KEGG) Database.

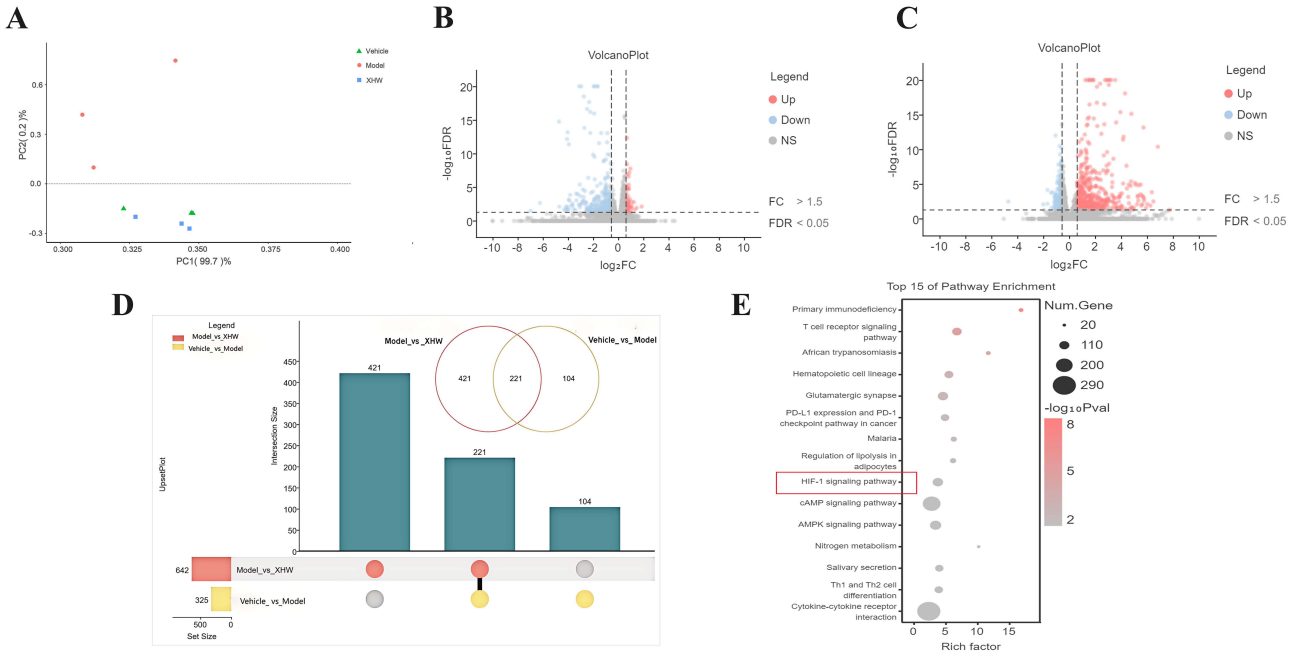

Figure 5 Analysis of differentially expressed genes (DEGs) in ICIs-related myocarditis improved by XHW. (**A**) PCA score plots from the vehicle, model and XHW groups. (**B**) Volcano plot of the vehicle group vs the model group. (**C**) Volcano plot of the model group vs the XHW group. (**D**) Venn diagram of DEGs between the vehicle vs model groups, the model vs the XHW groups. (**E**) KEGG enrichment analysis of DEGs revealed the top15 pathways significantly enriched in comparisons between the vehicle vs model groups, the model vs the XHW groups.

Differentially expressed genes (DEGs) with false discovery rate (FDR) < 0.05 and log2FC > 1 or < −1 were considered significant. This analysis revealed significant expression differences in 325 genes between the vehicle group and the model group, comprising 55 upregulated and 270 downregulated genes. The model group and the XHW group exhibited significant expression differences in 642 genes; 505 were upregulated, and 137 were downregulated (Figure 5B and C). To identify variables affected by XHW, we employed Venn diagrams to scrutinize the differentially expressed genes

across the vehicle, model, and XHW groups. Venn diagram analysis of differentially expressed variables between the vehicle, model, and XHW groups revealed 221 shared variables (Figure 5D and Table S4). These variables showed differential expression in both the vehicle-model and model-XHW comparisons.

To further investigate the crucial biological pathways through which XHW improves ICIs-related myocarditis, a pathway enrichment analysis was conducted on 221 DEGs using the KEGG database. In the KEGG analysis of DEGs, the top 15 significantly enriched pathways included the HIF-1 signaling pathway, which was enriched in the differential metabolite pathway (Figure 5E and Table S5). These findings indicate that the HIF-1 signaling pathway may serve as a significant regulatory pathway for XHW in improving ICIs-related myocarditis. The mRNA expression levels of genes related to the HIF-1 signaling pathway were determined by RT-PCR (Figure 6). The results confirmed that, compared to the vehicle group, the relative mRNA expression of HIF-1 was downregulated in the model group ($P<0.01$). Meanwhile, the relative mRNA expression of *Angpt1, Angpt2* ($P<0.01$), *Nppa* ($P<0.01$), and *Trf* ($P<0.05$) was upregulated. Compared to the model group, XHW upregulated *HIF-1* ($P<0.01$) and downregulated *Angpt1* ($P<0.05$), *Angpt2* ($P<0.05$), *Nppa* ($P<0.01$), *Trf* ($P<0.01$), and *Igf1* ($P<0.05$). This further validated the speculated improvement mechanism.

Correlation Analysis of Transcriptomics and Metabolomics

To further screen for metabolic markers associated with ICIs-induced myocarditis improved by XHW, we conducted a correlation analysis between key metabolites and differentially expressed genes in the HIF-1 signaling pathway. By analyzing the differential metabolites of the vehicle, model and XHW groups using Venn diagrams, we discovered that among the 31 variables, there is overlap between grbetween the vehicle vs model groups, the model vs the XHW groups (Figure 7A and Table S6). This suggests that these differential metabolites are closely linked to XHW's improvement of ICIs-induced myocarditis. Additionally, we performed a correlation analysis between these metabolites and differentially expressed genes (*Angpt1, Angpt2, Nppa, Trf, and Igf1*) on the HIF-1 signaling pathway. The correlation analysis network diagram for 31 metabolites and 5 genes is presented in Figure 7B. We also generated a correlation heatmap between the two, where the correlation strength between metabolites and DEGs is indicated by the Pearson correlation coefficient (Figure 7C). Metabolites Carnitine C3:0, Val-Asp-Pro-Val-Asn, H-Tyr-Pro-Phe-Val-Glu-Pro-Ille-OH, Urocanic acid, Thr-Val-Tyr-Lys-Gly, Leu-Glu-Lys-Glu, and Trp-Arg-Phe exhibited significant positive correlations with *Angpt1, Angpt2, Nppa, Trf, and Igf1*. Metabolites such as Glu-Phe-Tyr-Leu-Gly, Emetan (6′, 7′, 10, 11-tetramethoxy-), Asn-Val-Asp-Glu-Val, 13-Tetradecynoic acid, 1-Pentadecanoyl-glycerol, Arginyl-glycyl-aspartic acid, Pro-Val-Ala-Glu-Val, 3, 4-Dihydro-2, 7, 8-trimethyl-2-[(3E, 7E)-4, 8, 12-trimethyl-3, 7, 11-tridecatrienyl]-2H-1-benzopyran-6-ol, and Gln-Val-Leu-Leu-Gly exhibited a significant negative correlation with *Angpt1, Angpt2, Nppa, Trf, and Igf1*. Their content changes are illustrated in Figure 8. The trend of changes in the XHW group aligns with that of the control group, yet contrasts with the trend observed in the model group. In conclusion, these 16 metabolites are deemed as key metabolic markers for XHW in improving ICIs-related myocarditis.

Discussion

Although drugs targeting PD-1/PD-L1 have been employed as a novel cancer treatment strategy in clinical settings, the toxic effects of PD-1/PD-L1 inhibitors on the myocardium have constrained their broader clinical application. Cardiac troponin I (cTnI) is regarded as a specific cardiac antigen, contributing to the development of autoimmune cardiotoxicity.[28] In our study, we utilized a cTnI/PD-1-induced ICIs model.[26] We assessed the changes in cardiac function in each group of mice using an echocardiography system and detected biomarkers of myocardial injury in their serum. The results indicated that mice with ICIs-related myocarditis exhibited decreased LVEF and FS values, accompanied by increased plasma levels of CK and CK-MB, all of which confirmed the impairment of cardiac function in mice. However, after administering XHW, the LVEF and FS values of the mice, as well as the plasma levels of CK and CK-MB, all returned to normal, approaching those of normal mice. The research results indicate that XHW can improve the cardiac function of mice with myocarditis and alleviate myocardial damage caused by ICIs. N-Terminal Pro-B-Type Natriuretic Peptide (NT-proBNP) holds significant diagnostic value in identifying heart failure.[29] In terms of pathological correlation, CK and CK-MB are more sensitive indicators of myocardial injury.[30] Further testing is required in the future

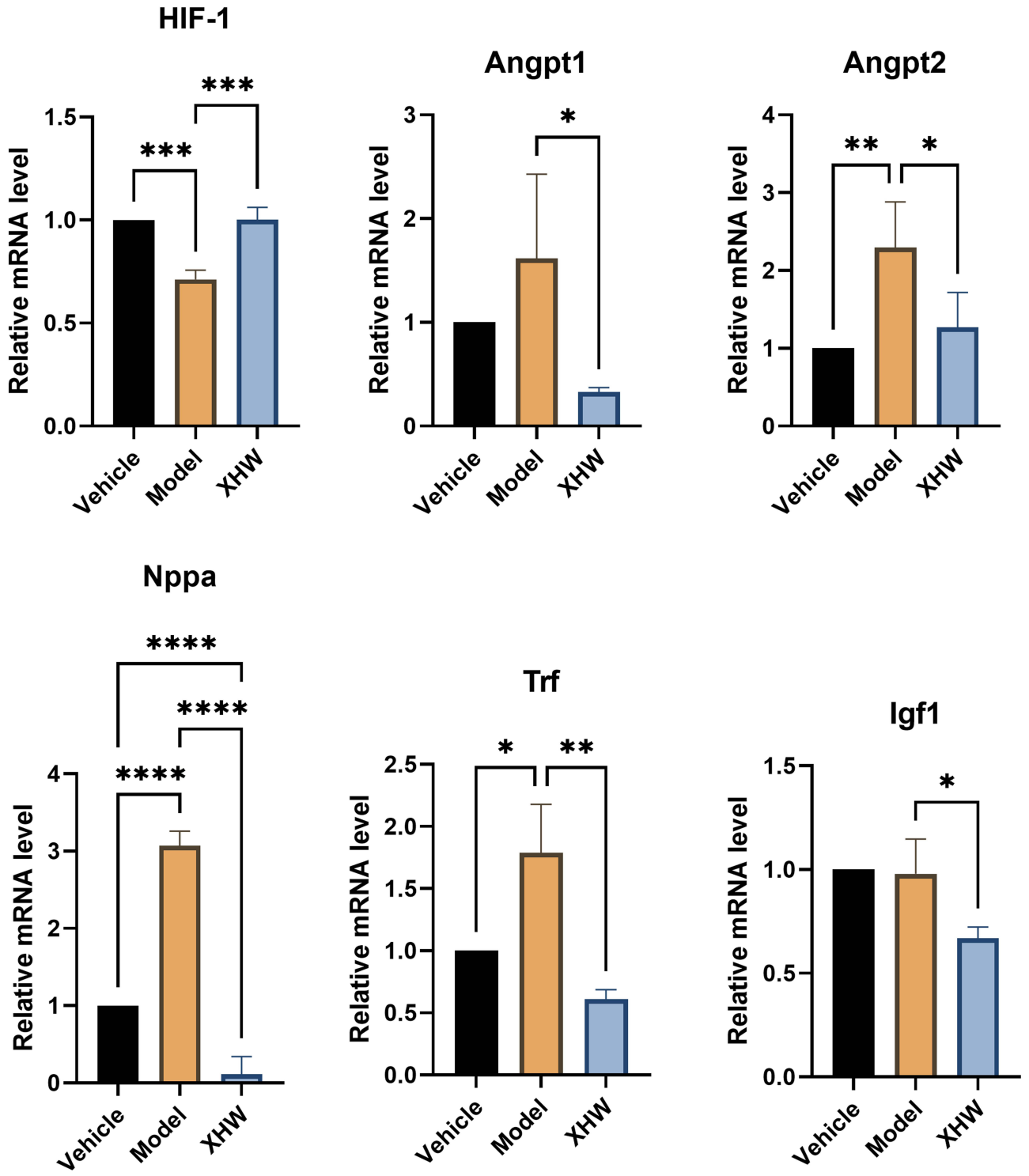

Figure 6 The relative mRNA levels of *HIF-1, Angpt1, Angpt2, Nppa, Trf* and *Igf1* in the cardiac, normalized to *β-actin*. Data are presented as the mean ± SD (n = 3). **P*< 0.05, ***P* < 0.01, ****P* < 0.001, and *****P* < 0.0001; model vs indicated groups.

to examine the impact of XHW on NT ProBNP levels in mice with ICIs-induced cardiotoxicity, in order to elucidate its role in heart failure. By integrating metabolomics and transcriptomics, it was revealed that XHW inhibits ICIs-related myocarditis by regulating the HIF-1 pathway, and the expression of HIF-1 pathway-related targets was validated by RT-

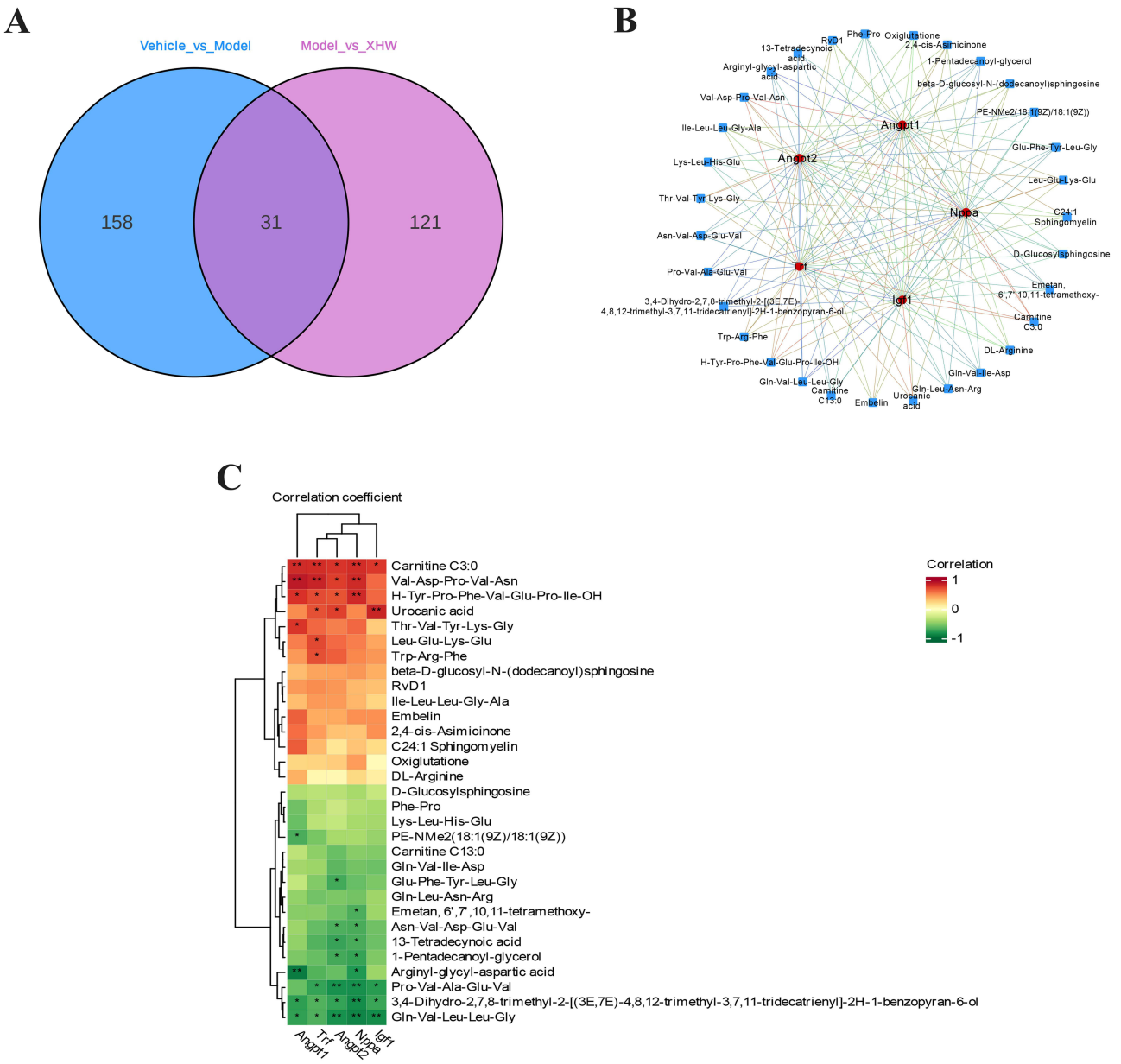

Figure 7 Correlation analysis of of transcriptomics and Metabolomics data. (**A**) Venn diagram of differentially expressed metabolites identified between the vehicle vs model groups, the model vs the XHW groups. (**B**) The correlation network of 5 DEGs and 31 metabolites. (**C**) The heatmap of correlation between 5 DEGs and 31 metabolites. **P*< 0.05, ***P* < 0.01.

PCR. In summary, we believe that XHW may protect the heart from damage by regulating the HIF-1 pathway, and can serve as a potential therapeutic drug for preventing ICIs-related myocarditis.

PD-1 inhibitor therapy disrupts immune homeostasis and induces metabolic disorders, ultimately compromising the integrity of the heart.[31] Hence, we explore the mechanism by which XHW improves ICIs-related myocarditis from a metabolomics perspective. Through screening for differential metabolites between the XHW group and the model group, and utilizing KEGG enrichment analysis, we identified the main enriched pathways as taurine and hypotaurine metabolism, ascorbate and aldarate metabolism, sphingolipid metabolism, and HIF−1 signaling pathway. Taurine and hypotaurine metabolism is closely linked to heart-related diseases and plays a role in the metabolic disorders associated with myocarditis.[32] Taurine, being the most abundant free amino acid in the myocardium, is essential for preserving the heart's structure and function. Studies indicate that taurine can shield the heart from toxic harm by mitigating oxidative

https://doi.org/10.2147/JIR.S527372

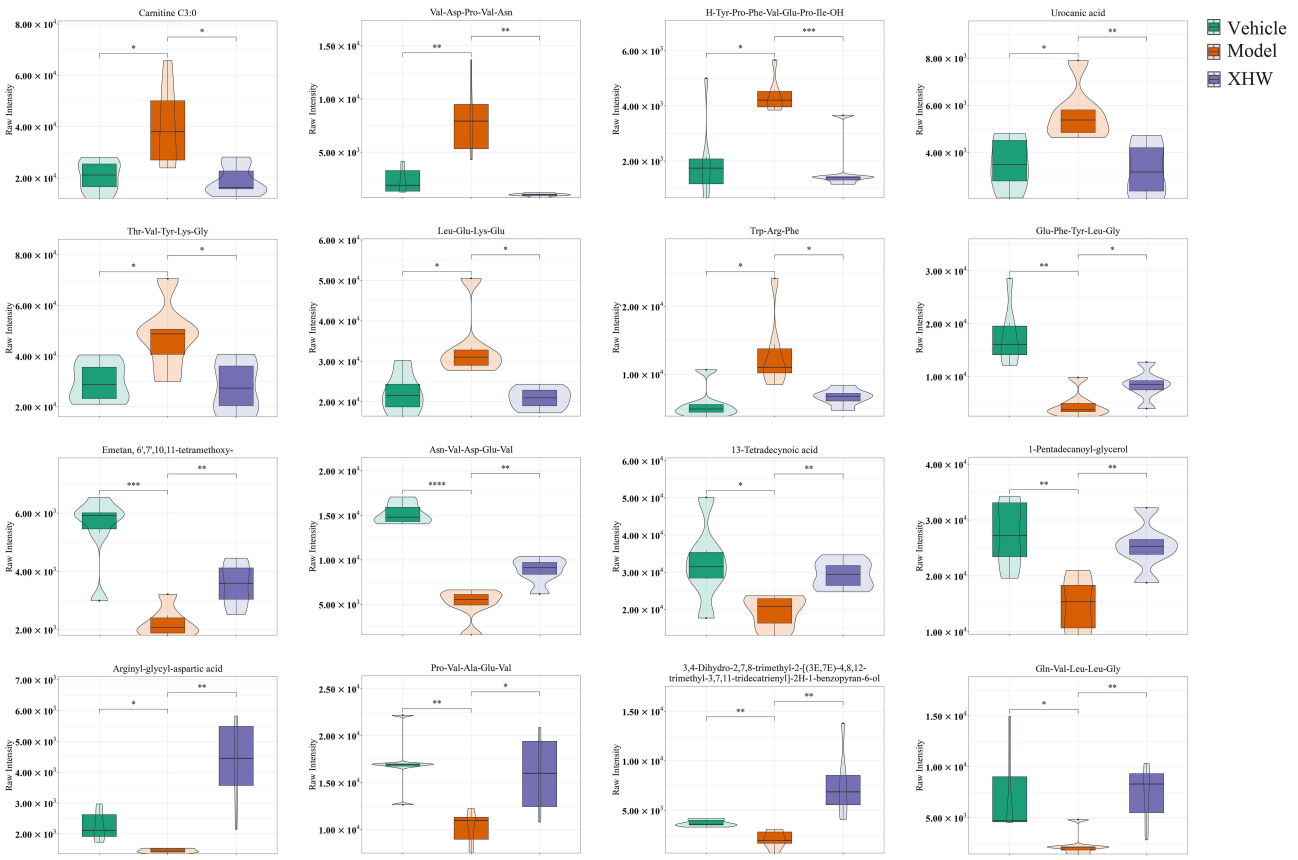

Figure 8 Violin plot of 16 differentially expressed metabolites significantly associated with 5 DEGs. Groupings are represented on the x-axis, while the y-axis shows the relative content of differential metabolites, expressed as original peak area. Data are presented as the mean ± SD (n = 6). **P*< 0.05, ***P* < 0.01, ****P* < 0.001, and *****P* < 0.0001; model vs indicated groups.

stress.[33] Sphingolipid metabolism profoundly affects cardiac function and structure, and can regulate mammalian cardiac regeneration.[34] Changes in sphingolipid metabolism can also mitigate cell death and inflammatory response after myocardial infarction.[35] HIF−1 signaling pathway plays a crucial role in heart disease.[36] Recent studies have revealed that HIF-1α inhibits the proliferation of cardiac fibroblasts by regulating reactive oxygen species (ROS) in mitochondria, ensuring that fibroblasts do not excessively proliferate and cause fibrosis in the event of myocardial infarction.[37] Currently, there are no relevant reports on the relationship between ascorbate and aldarate metabolism and heart disease, and further verification is required. Our results indicate that the regulation of metabolic disorders such as taurine and hypotaurine metabolism, sphingolipid metabolism, and HIF−1 signaling pathway by XHW may be a potential mechanism underlying XHW's ability to reduce ICIs-induced cardiac injury.

To further elucidate the specific biological mechanism by which XHW ameliorates ICIs-related cardiotoxicity, we screened for key differentially expressed genes via transcriptomics, focusing on those that contribute to XHW's reduction of ICIs-related cardiotoxicity. We then conducted pathway enrichment analysis using the KEGG database. Notably, our final enrichment results included HIF−1 signaling pathway, aligning with the results obtained from metabolomics analysis. Consequently, we hypothesize that HIF−1 signaling pathway represents a key pathway through which XHW mitigates ICIs-related cardiotoxicity. Through further RT-PCR experiments, we verified that the expression levels of key genes (*HIF-1, Nppa, Angpt1, Angpt2* and *Trf*) within HIF−1 signaling pathway align with the transcriptome findings. HIF-1 is crucial for myocardial protection, serving as a key biomarker associated with cardioprotection.[38] Mild hypoxia elicits HIF-1-mediated apoptosis inhibition, preserving myocardial viability, while prolonged, severe hypoxia triggers apoptosis to limit damage to surrounding myocardium.[39] In ischemic heart disease, sustained HIF-1 expression, amidst cellular hypoxia, facilitates binding to the vascular endothelial growth factor (VEGF) gene's hypoxia response element,

stimulating angiogenesis and improving myocardial perfusion.[40] Consistent with these results, this study's findings demonstrate elevated HIF-1 expression in both the XHW and control mouse groups compared to the model group. *Nppa* is one of the commonly used cardiac injury markers for heart failure in clinical practice, indicating the occurrence of the decompensated phase of dilated cardiomyopathy and the severity of heart failure symptoms.[41,42] This is consistent with the expression results of *Nppa* in different groups of mice in this study. *Angpt1* and *Angpt2* are angiopoietins crucial for vascular development and angiogenesis. *Angpt2*, a marker of vascular instability and poor prognosis in ischemic heart disease.[43,44] Recent research indicates that blocking *Angpt2* could potentially serve as a treatment option for ischemic heart failure.[45] Our study demonstrates that XHW reduces *Angpt2* expression. This study offers a novel strategy for the clinical treatment of cardiac dysfunction resulting from ICIs. Nevertheless, the study has its limitations. First, the precise mechanism by which XHW reduces cardiac toxicity from ICIs through the regulation of the HIF-1 signaling pathway requires further validation. Secondly, the pharmacodynamic substances and targets of XHW in mitigating cardiotoxicity induced by ICIs need to be clarified. Additionally, as a traditional Chinese medicine compound consisting of four herbs, the pharmacokinetics and bioavailability of XHW are relatively complex. Further research is required to clarify these aspects. Future research should incorporate multi-omics integrated analysis technology and preclinical safety evaluations to expedite the innovation of TCM in the adjunctive treatment of adverse reactions associated with ICIs.

Conclusion

In conclusion, this study integrated metabolomics and transcriptomics analysis to investigate the regulatory effects and therapeutic characteristics of XHW in the treatment of ICIs-related myocarditis. Our study provides evidence that XHW can mitigate ICIs-related cardiac toxicity by regulating the HIF-1 signaling pathway, which may offer a novel strategy for treating ICIs-induced cardiac dysfunction. Moreover, The findings provide a foundation for further research on XHW's potential in preventing and managing adverse reactions related to ICIs.

Data Sharing Statement

The original findings described in this study can be found in the article/Supplementary Material; for additional questions, please contact the corresponding authors.

Ethics Statement

Animal procedures were conducted in accordance with the National Institutes of Health guidelines for the care and use of laboratory animals, as approved by the Scientific Investigation Board of the Cancer Hospital, Chinese Academy of Medical Sciences, and in compliance with relevant ethical regulations of Peking Union Medical College.

Author Contributions

All authors made a significant contribution to the work reported, whether that is in the conception, study design, execution, acquisition of data, analysis and interpretation, or in all these areas; took part in drafting, revising or critically reviewing the article; gave final approval of the version to be published; have agreed on the journal to which the article has been submitted; and agree to be accountable for all aspects of the work.

Funding

This work was supported by Bethune Quest-Pharmaceutical Research Capacity Building Project (Z04JKM2023E040).

Disclosure

The authors affirm that the research was carried out without any potential conflict of interest arising from commercial or financial relationships.

References

1. Ascier to PA, Marincola FM. 2025: the Year of Anti-PD-1/PD-L1s Against Melanoma and Beyond. *EBioMedicine*. 2015;2(2):92–93. doi:10.1016/j.ebiom.2015.01.011

2. Topalian SL, Forde PM, Emens LA, Yarchoan M, Smith KN, Pardoll DM. Neoadjuvant immune checkpoint blockade: a window of opportunity to advance cancer immunotherapy. *Cancer Cell*. 2023;41(9):1551–1566. doi:10.1016/j.ccell.2023.07.011
3. Jing Y, Yang J, Johnson DB, Moslehi JJ, Han L. Harnessing big data to characterize immune-related adverse events. *Nat Rev Clin Oncol*. 2022;19(4):269–280. doi:10.1038/s41571-021-00597-8
4. Khan S, Gerber DE. Autoimmunity, checkpoint inhibitor therapy and immune-related adverse events: a review. *Semi Cancer Biol*. 2020;64:93–101. doi:10.1016/j.semcancer.2019.06.012
5. Lyon AR, López-Fernández T, Couch LS, et al. ESC Guidelines on cardio-oncology developed in collaboration with the European Hematology Association (EHA), the European Society for Therapeutic Radiology and Oncology (ESTRO) and the International Cardio-Oncology Society (IC-OS). *Eur Heart J*. 2022;43(41):4229–4361. doi:10.1093/eurheartj/ehac244
6. Cao W, Han S, Zhang P, et al. Immune checkpoint inhibitor-related myocarditis in patients with lung cancer. *BMC Cancer*. 2025;25(1):685. doi:10.1186/s12885-025-13997-1
7. Zhu H, Galdos FX, Lee D, et al. Identification of Pathogenic Immune Cell Subsets Associated With Checkpoint Inhibitor-Induced Myocarditis. *Circulation*. 2022;146(4):316–335. doi:10.1161/CIRCULATIONAHA.121.056730
8. Moslehi J, Lichtman AH, Galluzzi L, Kitsis RN. Immune checkpoint inhibitor-associated myocarditis: manifestations and mechanisms. *J Clin Invest*. 2021;131:1.
9. Lehmann LH, Cautela J, Palaskas N, et al. Clinical Strategy for the Diagnosis and Treatment of Immune Checkpoint Inhibitor-Associated Myocarditis: a Narrative Review. *JAMA Cardiol*. 2021;6(11):1329–1337. doi:10.1001/jamacardio.2021.2241
10. Wang Q, Jiao L, Wang S, et al. Adjuvant Chemotherapy with Chinese Herbal Medicine Formulas Versus Placebo in Patients with Lung Adenocarcinoma after Radical Surgery: a Multicenter, Randomized, Double-Blind, Placebo-Controlled Trial. *Biological Procedures Online*. 2020;22(1):5. doi:10.1186/s12575-020-00117-5
11. Li C, Niu M, Wang R, et al. The modulatory properties of Si Jun Zi Tang enhancing anticancer of gefitinib by an integrating approach. *Biomed Pharmacothe*. 2019;111:1132–1140. doi:10.1016/j.biopha.2018.12.026
12. Liao YH, Li CI, Lin CC, Lin JG, Chiang JH, Li TC. Traditional Chinese medicine as adjunctive therapy improves the long-term survival of lung cancer patients. *J Cancer Res Clin Oncol*. 2017;143(12):2425–2435. doi:10.1007/s00432-017-2491-6
13. Li C, Zheng Y, Niu D, et al. Effects of Traditional Chinese Medicine Injections for Anthracyclines-induced Cardiotoxicity: an Overview of Systematic Reviews and Meta-Analyses. *Integr Cancer Ther*. 2023;22:15347354231164753. doi:10.1177/15347354231164753
14. Zhou M, Wang W, Weng J, Lai Z. A Review on Probable Causes of Cardiotoxicity Caused by Common Cancer Drugs and the Role of Traditional Chinese Medicine in Prevention and Treatment. *Pharmacogenomics Personalized Med*. 2023;16:1067–1077. doi:10.2147/PGPM.S427585
15. Cao B, Wang S, Li R, et al. Xihuang Pill enhances anticancer effect of anlotinib by regulating gut microbiota composition and tumor angiogenesis pathway. *Biomed Pharmacothe*. 2022;151:113081. doi:10.1016/j.biopha.2022.113081
16. Wang Y, Wang W, Liu K, et al. The mechanism of Xihuang pills' intervention in the tumour immune microenvironment for the treatment of liver cancer based on the STAT3-PDL1 pathway. *J Ethnopharmacol*. 2024;331:118278. doi:10.1016/j.jep.2024.118278
17. Xu HB, Chen XZ, Wang X, Pan J, Yi-Zhuo Z, Zhou CH. Xihuang pill in the treatment of cancer: TCM theories, pharmacological activities, chemical compounds and clinical applications. *J Ethnopharmacol*. 2023;316:116699. doi:10.1016/j.jep.2023.116699
18. Hu ML, Liao QZ, Liu BT, et al. Xihuang pill ameliorates colitis in mice by improving mucosal barrier injury and inhibiting inflammatory cell filtration through network regulation. *J Ethnopharmacol*. 2024;319:117098. doi:10.1016/j.jep.2023.117098
19. Lv M, Ding R, Ma P, et al. Network Pharmacology Analysis on the Mechanism of Xihuangwan in Treating Rectal Cancer and Radiation Enteritis. *Curr Pharm Des*. 2024;30(9):683–701. doi:10.2174/0113816128287232240213105913
20. Thabet NM, Abdel-Rafei MK, Moustafa EM. Boswellic acid protects against Bisphenol-A and gamma radiation induced hepatic steatosis and cardiac remodelling in rats: role of hepatic PPAR-α/P38 and cardiac Calcineurin-A/NFATc1/P38 pathways. *Arch Physiol Biochem*. 2022;128(3):767–785. doi:10.1080/13813455.2020.1727526
21. Fu Y, Liu T, He S, et al. Ursolic acid reduces oxidative stress injury to ameliorate experimental autoimmune myocarditis by activating Nrf2/HO-1 signaling pathway. *Front Pharmacol*. 2023;14:1189372. doi:10.3389/fphar.2023.1189372
22. Elshazly SM, Dm AEM, Nassar NN. The selective 5-LOX inhibitor 11-keto-β-boswellic acid protects against myocardial ischemia reperfusion injury in rats: involvement of redox and inflammatory cascades. *Naunyn-Schmiedeberg's Arch Pharmacol*. 2013;386(9):823–833. doi:10.1007/s00210-013-0885-9
23. Chen M, Wang M, Yang Q, et al. Antioxidant effects of hydroxysafflor yellow A and acetyl-11-keto-β-boswellic acid in combination on isoproterenol-induced myocardial injury in rats. *IntJ Mol Med*. 2016;37(6):1501–1510. doi:10.3892/ijmm.2016.2571
24. du Sert N P, Ahluwalia A, Alam S, et al. Reporting animal research: explanation and elaboration for the ARRIVE guidelines 2.0. *PLoS biol*. 2020;18(7):e3000411. doi:10.1371/journal.pbio.3000411
25. Li S, Tajiri K, Yuan Z, et al. 4E-BP3 deficiency impairs dendritic cell activation and CD4(+) T cell differentiation and attenuates α-myosin-specific T cell-mediated myocarditis in mice. *Basic Res Cardiol*. 2025;120(1):225–240. doi:10.1007/s00395-024-01089-3
26. Zhang H, Lin J, Shen Y, Pan J, Wang C, Cheng L. Protective Effect of Crocin on Immune Checkpoint Inhibitors-Related Myocarditis Through Inhibiting NLRP3 Mediated Pyroptosis in Cardiomyocytes via NF-κB Pathway. *J Inflamm Res*. 2022;15:1653–1666. doi:10.2147/JIR.S348464
27. Li C, Chen W, Zhang M, et al. Modulatory effects of Xihuang Pill on lung cancer treatment by an integrative approach. *Biomed Pharmacothe*. 2020;130:110533. doi:10.1016/j.biopha.2020.110533
28. Bockstahler M, Fischer A, Goetzke CC, et al. Heart-Specific Immune Responses in an Animal Model of Autoimmune-Related Myocarditis Mitigated by an Immunoproteasome Inhibitor and Genetic Ablation. *Circulation*. 2020;141(23):1885–1902. doi:10.1161/CIRCULATIONAHA.119.043171
29. McKie PM, Burnett Jr JC. NT-proBNP: the Gold Standard Biomarker in Heart Failure. *J Am Coll Cardiol*. 2016;68(22):2437–2439. doi:10.1016/j.jacc.2016.10.001
30. Kehl DW, Iqbal N, Fard A, Kipper BA, De La Parra Landa A, Maisel AS. Biomarkers in acute myocardial injury. *Transl Res*. 2012;159(4):252–264. doi:10.1016/j.trsl.2011.11.002
31. Michel L, Helfrich I, Hendgen-Cotta UB, et al. Targeting early stages of cardiotoxicity from anti-PD1 immune checkpoint inhibitor therapy. *Eur Heart J*. 2022;43(4):316–329. doi:10.1093/eurheartj/ehab430

32. Kong Q, Gu J, Lu R, et al. NMR-Based Metabolomic Analysis of Sera in Mouse Models of CVB3-Induced Viral Myocarditis and Dilated Cardiomyopathy. *Biomolecules*. 2022;13(1):12. doi:10.3390/biom13010012
33. Schaffer S, Kim HW. Effects and Mechanisms of Taurine as a Therapeutic Agent. *Biomolecules Ther*. 2018;26(3):225–241. doi:10.4062/biomolther.2017.251
34. Ji X, Chen Z, Wang Q, et al. Sphingolipid metabolism controls mammalian heart regeneration. *Cell Metab*. 2024;36(4):839–56.e8. doi:10.1016/j.cmet.2024.01.017
35. Hadas Y, Vincek AS, Youssef E, et al. Altering Sphingolipid Metabolism Attenuates Cell Death and Inflammatory Response After Myocardial Infarction. *Circulation*. 2020;141(11):916–930. doi:10.1161/CIRCULATIONAHA.119.041882
36. Zhao Y, Xiong W, Li C, et al. Hypoxia-induced signaling in the cardiovascular system: pathogenesis and therapeutic targets. *Signal Transduct Target Ther*. 2023;8(1):431. doi:10.1038/s41392-023-01652-9
37. Janbandhu V, Tallapragada V, Patrick R, et al. Hif-1a suppresses ROS-induced proliferation of cardiac fibroblasts following myocardial infarction. *Cell Stem Cell*. 2022;29(2):281–97.e12. doi:10.1016/j.stem.2021.10.009
38. Hu Y, Lu H, Li H, Ge J. Molecular basis and clinical implications of HIFs in cardiovascular diseases. *Trends Mol Med*. 2022;28(11):916–938. doi:10.1016/j.molmed.2022.09.004
39. Yu B, Wang X, Song Y, et al. The role of hypoxia-inducible factors in cardiovascular diseases. *Pharmacol Ther*. 2022;238:108186. doi:10.1016/j.pharmthera.2022.108186
40. Wu J, Bond C, Chen P, et al. HIF-1α in the heart: remodeling nucleotide metabolism. *J Mol Cell Cardiol*. 2015;82:194–200. doi:10.1016/j.yjmcc.2015.01.014
41. Houweling AC, van Borren MM, Moorman AF, Christoffels VM. Expression and regulation of the atrial natriuretic factor encoding gene Nppa during development and disease. *Cardiovas Res*. 2005;67(4):583–593. doi:10.1016/j.cardiores.2005.06.013
42. Tripathi R, Sullivan RD, Fan TM, et al. Cardiac-Specific Overexpression of Catalytically Inactive Corin Reduces Edema, Contractile Dysfunction, and Death in Mice with Dilated Cardiomyopathy. *Int J Mol Sci*. 2019;21(1):203. doi:10.3390/ijms21010203
43. Lorbeer R, Baumeister SE, Dörr M, et al. Circulating angiopoietin-2, its soluble receptor Tie-2, and mortality in the general population. *Eur J Heart Failure*. 2013;15(12):1327–1334. doi:10.1093/eurjhf/hft117
44. Pöss J, Fuernau G, Denks D, et al. Angiopoietin-2 in acute myocardial infarction complicated by cardiogenic shock—a biomarker substudy of the IABP-SHOCK II -Trial. *Eur J Heart Failure*. 2015;17(11):1152–1160. doi:10.1002/ejhf.342
45. Lee SJ, Lee CK, Kang S, et al. Angiopoietin-2 exacerbates cardiac hypoxia and inflammation after myocardial infarction. *J Clin Invest*. 2018;128(11):5018–5033. doi:10.1172/JCI99659